3. Lattice vibration

7. Debye model

7.1 What is Debye model?

Debye model predicts the isochoric heat capacity C_V of crystals considering the frequency dependence of the number of modes as a function of temperature T, which is the most striking difference to Einstein model. Although there is a marked inconsistency between the Einstein model and experimental results in the low T region, the Debye model succeeds in showing a good agreement in the T dependence of C_V at low T ($C_V \propto T^3$) for many monatomic solids.

7.2 Lattice vibration

Crystal is an assemblage of atoms and lattices, which show thermal vibration. The thermal vibration generally shows very complicated wave form, but it can be decomposed into a superposition of longitudinal and transverse waves. The propagation direction of the first and second ones are parallel and perpendicular to the atomic/lattice displacements, respectively. In addition, transverse waves are constituted by two components with the different oscillation directions: horizontally and vertically oscillating ones. The waves can be further decomposed into a superposition of normal modes (simple harmonic motions). In order to count the number of modes, let us consider a one-dimensional (1D) model crystal (linear monatomic chain) with the periodic boundary condition as shown in Fig. 3.7.1. The periodic boundary condition is favorable for the system with translational symmetry such as crystal lattice. If we adopt other boundary conditions, the argument will be essentially the same. The 1D crystal contains N ($\gg 1$) atoms whose interval is a (constant), and there are interactions between adjacent atoms via a spring. The length of the crystal L is then given by

$$L = (N-1)a \approx Na. \tag{3.7.1}$$

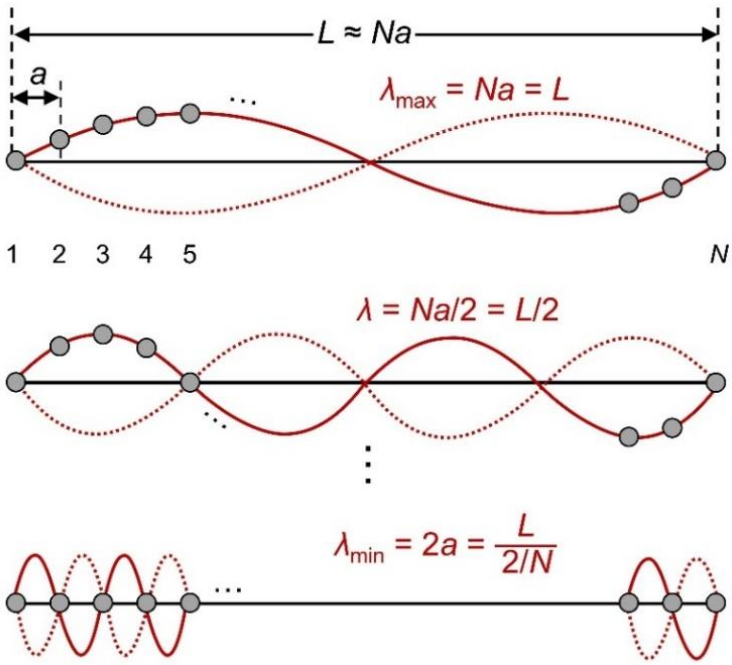

Fig. 3.7.1. Some normal modes for lattice vibration of the linear monatomic chain.

Then the 1D crystal has the modes with the following wavelengths λ and angular wavenumbers k:

$$L = Na(= \lambda_{\max}),\quad \frac{L}{2} = \frac{Na}{2},\quad \cdots\quad ,\quad 2a = \frac{2L}{N} = \frac{L}{N/2}(= \lambda_{\min}). \tag{3.7.2}$$

$$\pm\frac{2\pi}{L}(= k_{\min}),\quad \pm 2\frac{2\pi}{L},\quad \pm 3\frac{2\pi}{L},\quad \cdots\quad ,\quad \pm\frac{N}{2}\frac{2\pi}{L}(= k_{\max}). \tag{3.7.3}$$

Here, ± comes from two propagation directions (from left to right and the other way around). The sequence of $|k|$ has a constant interval of $2\pi/L$, and there are $2 \times N/2 = N$ modes in total. In addition, the number of modes is finite (section 3.6), because atoms vibrate in the equivalent phase when $\lambda < \lambda_{\min}$, i.e., $\lambda = a, a/2, a/4, \cdots$.

7.3 Density of states

Since we determined the wavenumber of the 1D crystal's modes in section 3.7.2, let us start this section from computing the density of states $D(\omega)$, which is essential for the heat capacity. $D(\omega)$ is the number of modes n_m at a given frequency ω, which is given by

$$D(\omega)\mathrm{d}\omega = \frac{\mathrm{d}n_m}{\mathrm{d}\omega}\mathrm{d}\omega = \frac{\mathrm{d}n_m}{\mathrm{d}k}\frac{\mathrm{d}k}{\mathrm{d}\omega}\mathrm{d}\omega. \tag{3.7.4}$$

Recall that the interval of $|k|$ is $2\pi/L$ (Eq. 3.7.3), $\mathrm{d}n_m/\mathrm{d}k$ turns into

$$\frac{\mathrm{d}n_m}{\mathrm{d}k} = \pm\frac{1}{2\pi/L} = \pm\frac{L}{2\pi}. \tag{3.7.5}$$

In order to derive $\mathrm{d}k/\mathrm{d}\omega$, let us obtain the dispersion relation. Assuming a linear relation between ω and k near $k = 0$ at low T (Fig. 3.7.2), one can approximate ω as a solution of the equation of motion for atoms in the 1D crystal:

$$\omega = \sqrt{\frac{4C}{m}}\left|\sin\left(\frac{ka}{2}\right)\right| \cong \sqrt{\frac{4C}{m}}\left|\frac{ka}{2}\right| = \sqrt{\frac{C}{m}}a|k|, \tag{3.7.6}$$

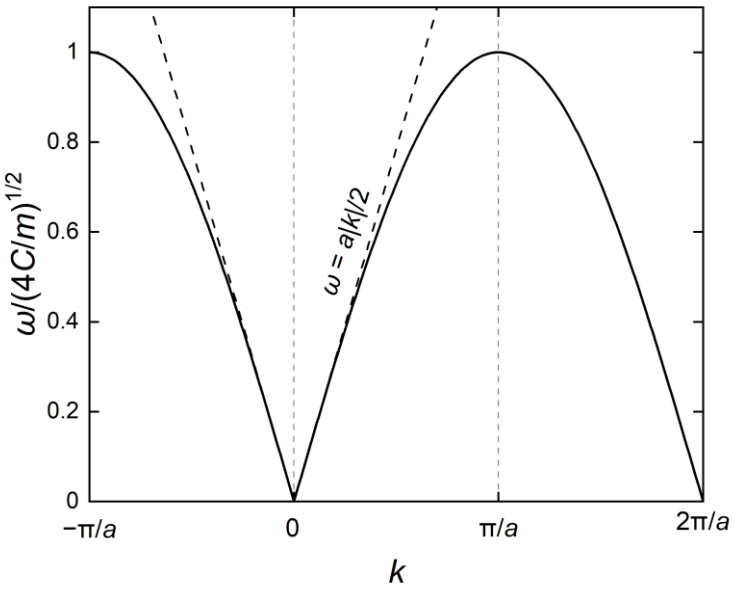

Fig. 3.7.2. Dispersion relation of the lattice vibration for the 1D crystal (solid curve). The black broken line indicates the linear dispersion relation assumed in Eq. (3.7.6). Due to the periodic boundary condition and the discrete configuration of atoms, the essential region is only $-\pi/a \le k < \pi/a$ (the first Brillouin zone).

where C and m are the spring constant and the atomic mass, respectively. Combining the definitions of group ($v_g \equiv d\omega/dk$) and phase ($v_p \equiv \omega/k$) velocities (section 3.5), and Eq. (3.7.6), we have

$$v_g \equiv \frac{d\omega}{dk} \approx \frac{\omega}{k} = \pm\sqrt{\frac{C}{m}}a \equiv v_p. \tag{3.7.7}$$

Then $dk/d\omega$ is

$$\frac{dk}{d\omega} = \frac{1}{v_g} \approx \frac{1}{v_p} = \pm\frac{1}{a}\sqrt{\frac{m}{C}}. \tag{3.7.8}$$

Substituting Eqs. (3.7.5) and (3.7.8) into Eq. (3.7.4), $D(\omega)$ (≥ 0) of the 1D crystal is

$$D(\omega) = \frac{dn_m}{dk}\frac{dk}{d\omega} \approx \left(\pm\frac{L}{2\pi}\right) \times \left(\pm\frac{1}{a}\sqrt{\frac{m}{C}}\right) = \frac{L}{2\pi a}\sqrt{\frac{m}{C}} = \text{const.} \tag{3.7.9}$$

It represents that $D(\omega)$ is independent of ω.

Let us move on to deriving $D(\omega)$ for the three-dimensional (3D) crystal. Its reciprocal lattice points are aligned with interval of $2\pi/L$ in 3D k-space (Fig. 3.7.3), as is the case of the 1D crystal. When we divide the 3D k-space into equal cubes including a lattice point (dashed red square in Fig. 3.7.3), its volume is

$$\left(\frac{2\pi}{L}\right)^3 = \frac{8\pi^3}{V}, \tag{3.7.10}$$

where V ($= L^3$) is the volume of the 3D crystal. Lattice points of interest are those only inside the sphere with a radius of k_{max} (dashed red circle in Fig. 3.7.3), whose volume is

$$V_{k \leq k_{max}} = \frac{4}{3}\pi k_{max}^3. \tag{3.7.11}$$

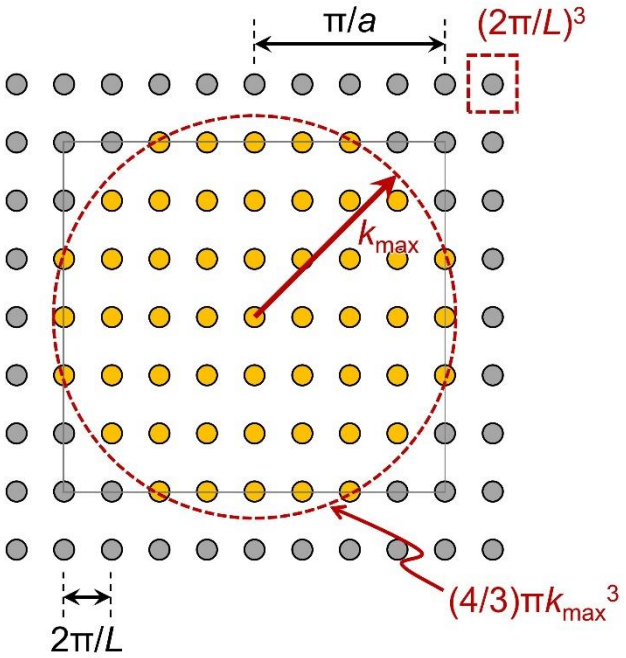

Fig. 3.7.3. Sliced k-space for the 3D model crystal lattice. The circles represent lattice points, where those within the spherical region: $|k| \leq k_{max}$ (dashed red circle) are shown by orange circles. The solid gray and the dashed red squares, respectively, indicate the first Brillouin zone and the unit volume containing a lattice point.

Combining Eqs. (3.7.10) and (3.7.11), we obtain the number of modes n_m (k-points) such that $|k| \leq k_{max}$:

$$n_m = \frac{(4/3)\pi k_{max}^3}{8\pi^3/V} = \frac{Vk_{max}^3}{6\pi^2}. \tag{3.7.12}$$

When V is large and a is small (i.e., k is large), n_m becomes greater. Based on the low-T approximation ($v_g \approx v_p$), one can derive $D(\omega)$ at given mode of the 3D crystal:

$$D(\omega) = \frac{dn_m}{d\omega} = \frac{dn_m}{dk}\frac{dk}{d\omega} = \frac{d}{dk}\left(\frac{Vk^3}{6\pi^2}\right)\frac{1}{v_g} = \frac{Vk^2}{2\pi^2 v_g} \approx \frac{Vk^2}{2\pi^2 v_p} = \frac{V(\omega/v_p)^2}{2\pi^2 v_p}$$

$$= \frac{V\omega^2}{2\pi^2 v_p^3} \propto \omega^2. \tag{3.7.13}$$

$D(\omega)$ of the 3D crystal depends on ω^2 up to ω_D, which is described in section 3.7.3 (Fig. 3.7.4b). n_m = 0 for any ω except for ω_α for the Einstein model (Fig. 3.7.4a). Sum $D(\omega)$ up for one longitudinal and two transverse waves,

$$D(\omega) = \frac{Vk^2}{2\pi^2 v_L^3} + \frac{2Vk^2}{2\pi^2 v_T^3} = \frac{3V\omega^2}{2\pi^2 v_D^3}. \tag{3.7.14}$$

Here, v_L and v_T are the group velocity of the longitudinal and transverse waves, respectively. Eq. (3.7.14) contains Debye sound velocity v_D, which is defined as follows:

$$\frac{3}{v_D^3} \equiv \frac{1}{v_L^3} + \frac{2}{v_T^3}. \tag{3.7.15}$$

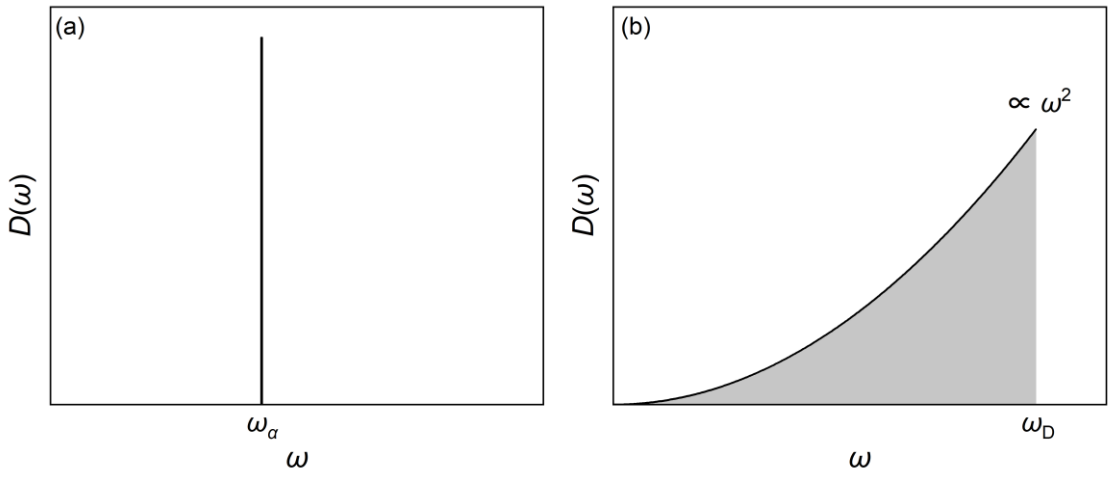

Fig. 3.7.4. A comparison of $D(\omega)$ between the Einstein (a) and the Debye (b) models. Here, ω_α indicates the Einstein frequency, which has a similar meaning in the Einstein model to that of ω_D. The horizontal and vertical axes are both in arbitrary units.

7.3 Total energy of lattice vibration

Since we have obtained $D(\omega)$ for the 3D-crystal (Eq. 3.7.14), now we have enough information to derive its total energy. Firstly, recall that the total energy of the lattice vibration E_{vib} is written as (see section 3.4)

$$E_{vib} = \int D(\omega)\frac{\hbar\omega}{e^{\hbar\omega/(k_B T)} - 1}d\omega, \tag{3.7.16}$$

where $\hbar$ and k_B are the reduced Planck constant and the Boltzmann constant, respectively. By substituting $D(\omega)$ (Eq. 3.7.14) into Eq. (3.7.16), one can show

$$E_{\mathrm{vib}} = \int_0^{\omega_{\mathrm{D}}} \frac{3V\omega^2}{2\pi^2 v_{\mathrm{D}}^3} \frac{\hbar\omega}{e^{\hbar\omega/(k_{\mathrm{B}}T)} - 1} \mathrm{d}\omega. \tag{3.7.17}$$

Again, the ω-range for the integration is limited to $0 \le \omega \le \omega_{\mathrm{D}}$ (Fig. 3.7.4b), since $|k| \le k_{\mathrm{max}} = \omega_{\mathrm{D}}/v_{\mathrm{D}}$. Here, ω_{D} is the Debye (cutoff) frequency. Assume that n_{m} satisfying $|k| \le k_{\mathrm{max}}$ is equal to the total number of atoms in the 3D crystal N,

$$N = n_{\mathrm{m}} = \frac{Vk_{\mathrm{max}}^3}{6\pi^2} = \frac{V\omega_{\mathrm{D}}^3}{6\pi^2 v_{\mathrm{D}}^3},$$

$$\therefore \omega_{\mathrm{D}} = v_{\mathrm{D}} \left(\frac{6\pi^2 N}{V}\right)^{\frac{1}{3}}. \tag{3.7.18}$$

This assumption is based on the idea that vibrational modes such that $|k| > k_{\mathrm{max}}$ does not exist (Fig. 3.7.4) and so does not contribute to E_{vib}. In order to simplify E_{vib}, let us define $x \equiv \hbar\omega/k_{\mathrm{B}}T$, and then we have $\omega = k_{\mathrm{B}}Tx/\hbar$ and $\mathrm{d}\omega = (k_{\mathrm{B}}T/\hbar)\mathrm{d}x$. If $\omega = \omega_{\mathrm{D}}$, x becomes x_{D} given by

$$x_{\mathrm{D}} = \frac{\hbar\omega_{\mathrm{D}}}{k_{\mathrm{B}}} \frac{1}{T} = \frac{\Theta_{\mathrm{D}}}{T}. \tag{3.7.19}$$

where Θ_{D} ($\equiv \hbar\omega_{\mathrm{D}}/k_{\mathrm{B}}$) is Debye temperature. By using x and x_{D}, one can rewrite Eq. (3.7.17) as

$$E_{\mathrm{vib}} = \int_0^{x_{\mathrm{D}}} \frac{3V(k_{\mathrm{B}}Tx/\hbar)^2}{2\pi^2 v_{\mathrm{D}}^3} \frac{k_{\mathrm{B}}Tx}{e^x - 1} \frac{k_{\mathrm{B}}T}{\hbar} \mathrm{d}x$$

$$= \frac{3Vk_{\mathrm{B}}^4 T^4}{2\pi^2 v_{\mathrm{D}}^3 \hbar^3} \int_0^{x_{\mathrm{D}}=\Theta_{\mathrm{D}}/T} \frac{x^4}{e^x - 1} \mathrm{d}x. \tag{3.7.20}$$

Now we can describe E_{vib} in the simple and convenient form that only contains x as an explicit parameter.

Let us clarify the physical meaning of Θ_{D}. Using Eq. (3.7.18), we can write Θ_{D} as follows:

$$\Theta_{\mathrm{D}} = \frac{\hbar\omega_{\mathrm{D}}}{k_{\mathrm{B}}} = \frac{\hbar v_{\mathrm{D}}}{k_{\mathrm{B}}} \left(\frac{6\pi^2 N}{V}\right)^{\frac{1}{3}}. \tag{3.7.21}$$

Eq. (3.7.21) tells that low-ω (i.e., low-E) states are dominant and high-ω states are not exited at low T. The higher-ω states are increasingly fill the energy levels at higher T. ω of excited modes reaches ω_{D} at Θ_{D}, above which all modes of lattice vibration become excited. Looking at the parameters of Θ_{D}, v_{D} (elastic moduli and density) and $N/V = 1/a^3$ (number density) are intrinsic for materials and others are universal constants. Thus, Θ_{D} is a specific constant to materials. Θ_{D} is high when v_{D} is high (rigid and light) and a is small (densely packed atoms). Therefore, Θ_{D} is an index of the T dependence of the vibrational properties for materials whose sound velocity and number density are different to each other. Since Θ_{D} is temperature literally, plotting the vibrational properties against the normalized temperature ($T/\Theta_{\mathrm{D}} = x_{\mathrm{D}}^{-1}$) is an effective measure to compare the vibrational properties for various materials.

7.5 Debye heat capacity

Now we are ready for deriving the Debye heat capacity C_{vib} by using the obtained E_{vib} and Θ_{D}. Since C_{vib} is a T derivative of E_{vib} (Eq. 3.7.17),

$$C_{\mathrm{vib}} \equiv \frac{\mathrm{d}E_{\mathrm{vib}}}{\mathrm{d}T} = \int_0^{\omega_{\mathrm{D}}} \frac{3V\omega^2}{2\pi^2 v_{\mathrm{D}}^3} \frac{\mathrm{d}}{\mathrm{d}T} \frac{\hbar\omega}{e^{\hbar\omega/(k_{\mathrm{B}}T)} - 1} \mathrm{d}\omega$$

$$= \int_0^{\omega_{\mathrm{D}}} \frac{3V\omega^2}{2\pi^2 v_{\mathrm{D}}^3} \frac{\hbar^2\omega^2 e^{\hbar\omega/(k_{\mathrm{B}}T)}}{k_{\mathrm{B}}T^2 (e^{\hbar\omega/(k_{\mathrm{B}}T)} - 1)^2} \mathrm{d}\omega$$

$$= \frac{3V\hbar^2}{2\pi^2 v_\mathrm{D}^3 k_\mathrm{B} T^2} \int_0^{\omega_\mathrm{D}} \frac{\omega^4 e^{\hbar\omega/(k_\mathrm{B}T)}}{(e^{\hbar\omega/(k_\mathrm{B}T)} - 1)^2} \mathrm{d}\omega. \tag{3.7.22}$$

Apply $\omega = k_\mathrm{B}Tx/\hbar$ and $\mathrm{d}\omega = (k_\mathrm{B}T/\hbar)\mathrm{d}x$ to Eq. (3.7.22)

$$C_\mathrm{vib} = \frac{3V\hbar^2}{2\pi^2 v_\mathrm{D}^3 k_\mathrm{B} T^2} \int_0^{x_\mathrm{D}} \frac{(k_\mathrm{B}Tx/\hbar)^4 e^x}{(e^x - 1)^2} \frac{k_\mathrm{B}T}{\hbar} \mathrm{d}x$$

$$= \frac{3V\hbar^2}{2\pi^2 v_\mathrm{D}^3 k_\mathrm{B} T^2} \left(\frac{k_\mathrm{B}T}{\hbar}\right)^5 \int_0^{x_\mathrm{D}} \frac{x^4 e^x}{(e^x - 1)^2} \mathrm{d}x$$

$$= \frac{9Nk_\mathrm{B}}{6\pi^2} \frac{1}{N/V} \left(\frac{k_\mathrm{B}T}{\hbar v_\mathrm{D}}\right)^3 \int_0^{x_\mathrm{D}} \frac{x^4 e^x}{(e^x - 1)^2} \mathrm{d}x$$

$$= 9Nk_\mathrm{B} \left\{\frac{k_\mathrm{B}T}{\hbar v_\mathrm{D} (6\pi^2 N/V)^{1/3}}\right\}^3 \int_0^{x_\mathrm{D}} \frac{x^4 e^x}{(e^x - 1)^2} \mathrm{d}x. \tag{3.7.23}$$

Eq. (3.7.23) becomes convenient with helps of Eqs. (3.7.19) and (3.7.21):

$$C_\mathrm{vib} = 9Nk_\mathrm{B} \left(\frac{T}{\Theta_\mathrm{D}}\right)^3 \int_0^{\Theta_\mathrm{D}/T} \frac{x^4 e^x}{(e^x - 1)^2} \mathrm{d}x \tag{3.7.24}$$

$$= \frac{9Nk_\mathrm{B}}{x_\mathrm{D}^3} \int_0^{x_\mathrm{D}} \frac{x^4 e^x}{(e^x - 1)^2} \mathrm{d}x. \tag{3.7.24'}$$

Now we would like to see that the behavior of C_vib under extreme T conditions. In the limit $T \to \infty$ and $x \to +0$,

$$C_\mathrm{vib} = \frac{9Nk_\mathrm{B}}{x_\mathrm{D}^3} \int_0^{x_\mathrm{D}} \frac{x^4 e^x}{(e^x - 1)^2} \mathrm{d}x \xrightarrow{x \to +0} \frac{9Nk_\mathrm{B}}{x_\mathrm{D}^3} \int_0^{x_\mathrm{D}} \frac{x^4}{x^2} \mathrm{d}x = \frac{9Nk_\mathrm{B}}{x_\mathrm{D}^3} \int_0^{x_\mathrm{D}} x^2 \mathrm{d}x = 3Nk_\mathrm{B}, \tag{3.7.25}$$

where we used

$$e^x \xrightarrow{x \to +0} 1, \tag{3.7.26}$$

$$e^x - 1 = x + \frac{1}{2!}x^2 + \frac{1}{3!}x^3 + \cdots \xrightarrow{x \to +0} x - 1 \to x. \tag{3.7.27}$$

The high-T limit of C_vib is consistent with Dulong-Petit law and this result manifests that all modes are excited. On the other hand, taking the limit $T \to +0$, $x_\mathrm{D} \to \infty$,

$$C_\mathrm{vib} = \frac{9Nk_\mathrm{B}}{x_\mathrm{D}^3} \int_0^{x_\mathrm{D}} \frac{x^4 e^x}{(e^x - 1)^2} \mathrm{d}x \xrightarrow{x_\mathrm{D} \to \infty} \frac{9Nk_\mathrm{B}}{x_\mathrm{D}^3} \frac{4\pi^4}{15} = \frac{12\pi^4 Nk_\mathrm{B}}{5} \left(\frac{T}{\Theta_\mathrm{D}}\right)^3 \propto T^3, \tag{3.7.28}$$

where, the following is used:

$$\int_0^\infty \frac{x^4 e^x}{(e^x - 1)^2} \mathrm{d}x = \Gamma(5)\zeta(4) = 4! \times \frac{\pi^4}{90} = \frac{4\pi^4}{15}. \tag{3.7.29}$$

Here, $\Gamma(\cdot)$ and $\zeta(\cdot)$ are gamma and Riemann zeta functions, respectively (see Appendix A for the detailed derivation of Eq. (3.7.29)). The Debye heat capacity is in much better agreement with experiments than $C_{V,\mathrm{Es}}$ at low T (Fig. 3.7.5). Eq. (3.7.28) tells that C_vib is proportional to T^3 at low T (Debye T^3 law). This law holds true because the number of excited atoms depends on T^3 (see Appendix B for details). However, C_vib deviate from the experimental data below ~6 K, as can be seen in the data for copper (transition metal). This is caused by the contribution to thermal conductivity from electrons increases with decreasing T. Contrastively, the Debye model matches the experiments better for diamond and lead (main-group elements).

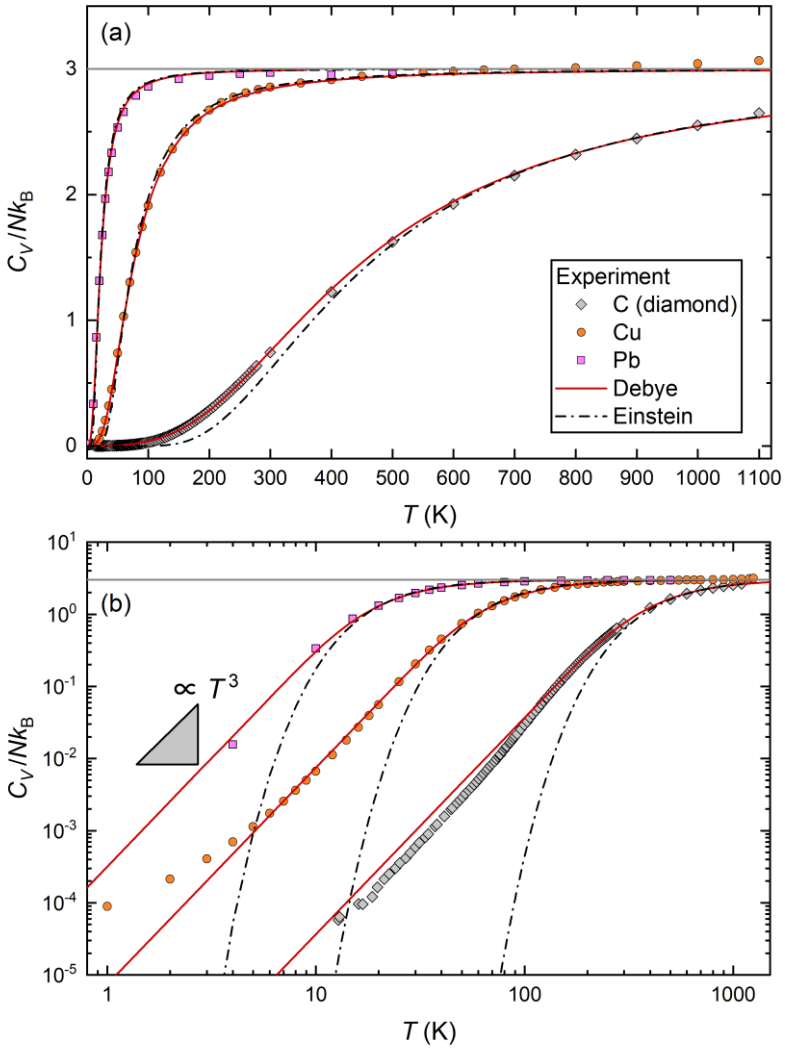

Fig. 3.7.5. Comparisons of the experimental data to the Debye and the Einstein models for the molar isochoric heat capacity (C_V/Nk_B) of C (diamond) (Desnoyehs and Morrison, 1958; Victor, 1962), Cu (White and Collocott, 1984), and Pb (Stedman et al., 1967) in linear (a) and logarithmic (b) representations. The horizontal gray line at $C_V/Nk_B = 3$ indicates the Dulong-Petit limit. The gray triangle in (b) is an eye guide for the dependence on T^3.

Let us compare C_{vib} and $C_{V,Es}$ at low T and consider the cause of difference. C_{vib} is higher than $C_{V,Es}$ at lower T (Fig. 3.7.5). Since the Einstein model considers only one frequency (Fig. 3.7.4a) and the low-E mode is absent, atoms are more unlikely to excite at low T. In contrast, the Debye model considers various frequencies (Fig. 3.7.4b), and hence, atoms can excite even at low T. Let us quantitatively consider the cause of this difference by comparing the average quantum number of quantum harmonic oscillators $\langle n \rangle$. In the case of copper, for example, Θ_D = 347 K (Stewart, 1983) and so $\omega_D = 4.5 \times 10^{13}$ Hz. The Einstein frequency of copper is $\omega_\alpha = 3.0 \times 10^{13}$ Hz, and so its Einstein temperature is $T_\alpha = 229$ K. ω_α is obtained by fitting $C_{V,Es}$ to the experimental data (White and Collocott, 1984), where $C_{V,Es}$ is given by

$$C_{V,\mathrm{Es}} = 3Nk_\mathrm{B}\left(\frac{T_\alpha}{T}\right)^2 \frac{e^{T_\alpha/T}}{(e^{T_\alpha/T}-1)^2} = 3Nk_\mathrm{B}\left(\frac{\hbar\omega_\alpha}{k_\mathrm{B}T}\right)^2 \frac{e^{\hbar\omega/(k_\mathrm{B}T)}}{(e^{\hbar\omega/(k_\mathrm{B}T)}-1)^2}. \quad (3.7.30)$$

Using these parameters, let us compare $\langle n \rangle$ for the Debye and the Einstein models. $\langle n \rangle$ is given by

$$\langle n\rangle = \frac{1}{e^{\hbar\omega/(k_B T)} - 1}. \tag{3.7.31}$$

As shown in Fig. 3.7.6, $\langle n\rangle$ for the Debye model at low ω (i.e., low T) is much larger than that for the Einstein model. One can compute C_V as

$$C_V \equiv \frac{\mathrm{d}E}{\mathrm{d}T} \propto \frac{\mathrm{d}}{\mathrm{d}T}\int D(\omega)\langle n\rangle \mathrm{d}x, \tag{3.7.32}$$

and hence, C_{vib} becomes larger at low T. In addition, the much larger area $\int D(\omega)\mathrm{d}\omega$ for the Debye model (Fig. 3.7.4) also makes C_{vib} larger, although it is difficult to discuss quantitatively.

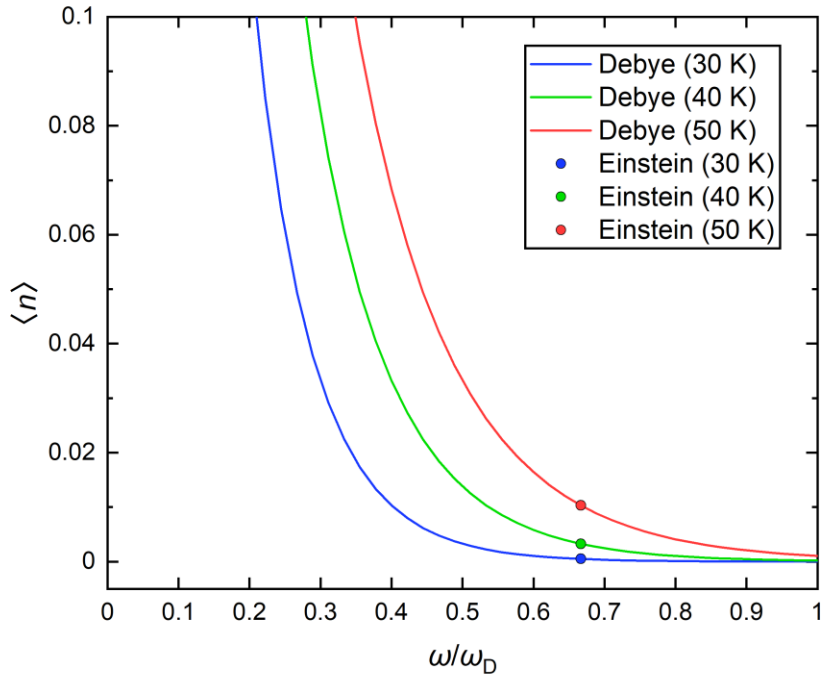

Fig. 3.7.6. Comparisons of the average quantum number $\langle n\rangle$ between the Debye and the Einstein models for copper at low T.

When we compare the Debye model to experiments for some rock-forming minerals, how these are consistent with each other varies with composition and/or crystal structure. In the case of simple oxides such as periclase and corundum (Kieffer, 1979), the Debye model generally matches the measurements, except for a slight underestimation in the intermediate T-range. The deviation suggests that, in these real crystals, all modes are excited at Θ_D (Θ_D = 910 K for periclase and Θ_D = 1036 K for corundum) and the average energy level filled by modes is higher than expected from the Debye model. When we look at the heat capacity for some orthosilicates such as forsterite and pyrope (Kieffer, 1980), the Debye model generally agrees to the experiments as well. But the Debye model slightly overestimates C_V above ~200 K, implying that a small proportion of modes are not excited at Θ_D (Θ_D = 756 K for forsterite and Θ_D = 794 K for pyrope). However, C_V of some tectosilicates such as quartz and albite (Kieffer, 1979) are poorly predicted by the Debye model. The Debye model largely overestimates C_V above ~50–100 K, suggesting that many of modes are not excited even above Θ_D (Θ_D = 560 K for quartz and Θ_D = 472 K for albite). Thus, atoms need more energy to excite lattice vibration than expected from elasticity.

Strictly speaking, Eq. (3.7.24') is just an interpolant for the heat capacity. The behavior of C_V at extreme temperatures (the Debye T^3 law and Dulong-Petit law) reflects the essence of the lattice vibration and is ubiquitous for various crystals. However, C_V at intermediate T condition is sensitive to the applied model and individual properties of crystals (e.g., composition, crystal structure). Eq. (3.7.24') only provides us with C_V as a rigid result of model calculation for the system with the idealized

lattice vibration. Hence, we cannot expect that the Debye model produces the enough precise C_V for real crystals which have complicated structure and interatomic potential.

7.6 Appendix A: Derivation of Eq. (3.7.29)

This section deals with the detailed calculations of Eq. (3.7.29). Firstly, $\Gamma(n+1)$ and $\zeta(n)$ are, respectively, defined as

$$\Gamma(n+1) = \int_0^\infty t^n e^{-t} \mathrm{d}t = n\Gamma(n) = n!, \tag{3.7.33}$$

$$\zeta(n) = \sum_{s=1}^{\infty} \frac{1}{s^n}. \tag{3.7.34}$$

Here, n and s are both natural numbers. We rewrite $\Gamma(n+1)$ as follows by substituting $t = sx$:

$$\Gamma(n+1) = \int_0^\infty (sx)^n e^{-sx} s\mathrm{d}x = s^n \int_0^\infty x^n s e^{-sx} \mathrm{d}x, \tag{3.7.35}$$

$$\therefore \frac{1}{s^n} = \frac{1}{\Gamma(n+1)} \int_0^\infty x^n s e^{-sx} \mathrm{d}x. \tag{3.7.36}$$

Substitute Eq. (3.7.36) into Eq (3.7.34),

$$\zeta(n) = \sum_{s=1}^{\infty} \frac{1}{\Gamma(n+1)} \int_0^\infty x^n s e^{-sx} \mathrm{d}x$$

$$= \frac{1}{\Gamma(n+1)} \int_0^\infty x^n \sum_{s=1}^{\infty} s e^{-sx} \mathrm{d}x. \tag{3.7.37}$$

Here, the infinite series in Eq. (3.7.37) is expanded as

$$\sum_{s=1}^{\infty} s e^{-sx} = e^{-x} + 2e^{-2x} + 3e^{-3x} + \cdots. \tag{3.7.38}$$

Multiplying both sides of Eq. (3.7.38) by e^x,

$$e^x \sum_{s=1}^{\infty} s e^{-sx} = 1 + 2e^{-x} + 3e^{-2x} + 4e^{-3x} + \cdots. \tag{3.7.39}$$

Subtracting Eq. (3.7.38) from Eq. (3.7.39),

$$(e^x - 1) \sum_{s=1}^{\infty} s e^{-sx} = 1 + e^{-x} + e^{-2x} + e^{-3x} + \cdots$$

$$= 1 + \sum_{s=1}^{\infty} e^{-sx} = 1 + \frac{e^{-x}}{1 - e^{-x}} = \frac{e^x}{e^x - 1}, \tag{3.7.40}$$

$$\therefore \sum_{s=1}^{\infty} s e^{-sx} = \frac{e^x}{(e^x - 1)^2}. \tag{3.7.41}$$

Combining Eqs. (3.7.37) and (3.7.41), we find

$$\zeta(n) = \frac{1}{\Gamma(n+1)} \int_0^\infty \frac{x^n e^x}{(e^x - 1)^2} \mathrm{d}x, \tag{3.7.42}$$

$$\therefore \Gamma(n+1)\zeta(n) = \int_0^\infty \frac{x^n e^x}{(e^x-1)^2}\,\mathrm{d}x. \tag{3.7.43}$$

If n = 4, we have Eq. (3.7.28) by using $\Gamma(n+1) = n!$ (Eq. 3.7.33) and $\zeta(4) = \pi^4/90$ (the derivation is omitted). $\zeta(4)$ can be computed by deriving Fourier series of the function $f(x) = x^2$ and by substituting the obtained Fourier coefficients into Parseval's identity.

7.7 Appendix B: Why the Debye T^3 law holds true?

This section is dedicated to giving a rough evaluation why C_V is proportional to T^3 at low T. Let a crystal be at enough low T that satisfies $T \ll \hbar\omega_D/k_B$ and let us assume $v_T \approx v_L \approx v_D$. By the way, it is known that $v_L \approx \sqrt{3}v_T$ and thus $v_D \approx 1.36v_T$ for Earth-forming rocks. Even at such low T, not all harmonic oscillators do not 'feel' cold. Whether the system is hot or cold for oscillators is rather dependent on the frequency for each oscillator. In this case, the system is cold for the oscillators such that $\omega \gtrsim k_BT/\hbar$, while the system is hot for those satisfying $\omega \lesssim k_BT/\hbar$. Let us roughly estimate C_{vib} based on this point of view. Since only excited modes contribute to the heat capacity, we need to obtain the number of excited modes (n_{active}). One can rewrite the condition such that the oscillators feel hot by using the dispersion relation at low T: $\omega \approx v_D|k| \lesssim k_BT/\hbar$, and hence, $|k| \lesssim k_BT/(\hbar v_D)$. Thus, as we derived Eq. (3.7.12), we can similarly approximate n_{active} as follows:

$$n_{\mathrm{active}} \sim \frac{(4/3)\pi(k_BT/\hbar v_D)^3}{8\pi^3/V} = \frac{k_B^3VT^3}{6\pi^2\hbar^3v_D^3}. \tag{3.7.44}$$

Assume that each excited oscillator has a heat capacity of approximately k_B, C_{vib} can be estimated as

$$C_{\mathrm{vib}} \sim 3n_{\mathrm{active}}k_B \sim \frac{k_B^4VT^3}{2\pi^2\hbar^3v_D^3}, \tag{3.7.45}$$

where the tripling comes from three oscillation directions of the modes. Here, recall that Eq. (3.7.28) is rewritten as follows with the help of Eq. (3.7.21):

$$\lim_{x_D\to\infty} C_{\mathrm{vib}} = \frac{12Nk_B\pi^4}{5}\left(\frac{T}{\Theta_D}\right)^3 = \frac{2\pi^2k_B^4VT^3}{5\hbar^3v_D^3}. \tag{3.7.28'}$$

Albeit the very rough evaluation, Eq. (3.7.45) matches Eq. (3.7.28') well in terms of dependencies between C_{vib} and each parameter. Therefore, we conclude that the Debye T^3 law works for low-T crystals because the number of excited oscillators is proportional to T^3.

7.9 References

Desnoyehs, J.E., Morrison, J.A., 1958. The heat capacity of diamond between 12·8° and 277°k. Philos. Mag. J. Theor. Exp. Appl. Phys. 3, 42–48. https://doi.org/10.1080/14786435808243223

Kieffer, S.W., 1980. Thermodynamics and lattice vibrations of minerals: 4. Application to chain and sheet silicates and orthosilicates. Rev. Geophys. 18, 862–886. https://doi.org/10.1029/RG018i004p00862

Kieffer, S.W., 1979. Thermodynamics and lattice vibrations of minerals: 3. Lattice dynamics and an approximation for minerals with application to simple substances and framework silicates. Rev. Geophys. 17, 35–59. https://doi.org/10.1029/RG017i001p00035

Stedman, R., Almqvist, L., Nilsson, G., 1967. Phonon-Frequency Distributions and Heat Capacities of Aluminum and Lead. Phys. Rev. 162, 549–557. https://doi.org/10.1103/PhysRev.162.549

Stewart, G.R., 1983. Measurement of low-temperature specific heat. Rev. Sci. Instrum. 54, 1–11. https://doi.org/10.1063/1.1137207

Victor, A.C., 1962. Heat Capacity of Diamond at High Temperatures. J. Chem. Phys. 36, 1903–1911. https://doi.org/10.1063/1.1701288

White, G.K., Collocott, S.J., 1984. Heat Capacity of Reference Materials: Cu and W. J. Phys. Chem. Ref. Data 13, 1251–1257. https://doi.org/10.1063/1.555728